Free-Space Optical Communication Link With Liquid Crystal Beam-Steering

Guanxiong Zhang, Andy Schreier, Xiuze Wang, William Matthews, James Farmer, Grahame Faulkner, Steve J. Elston, Stephen M. Morris, and Dominic O'Brien, *Member, IEEE*

***Abstract*— In this letter, we present a non-mechanical 2D beam-steering system suitable for optical wireless communication. Steering is achieved using polarization gratings combined with nematic liquid crystal cells operating as voltage-controlled polarization shifters. These steering elements are combined with a holographic diffuser matched to the discrete steering angles of the polarization grating, enabling continuous angular coverage. Beam-steering is also used at the receiver, allowing a large collection area receiver with a relatively narrow field of view to be used. The approach presented here could, in principle, be applied to a broad range of wavelengths (including visible light and near-infrared wavelengths). Furthermore, the technique does not inherently limit the transmission data rate. Besides, it improves the link margin and offers the potential for a bidirectional steered link using the same beam-steering elements. Details of the approach are set out in the letter, followed by experimental results from a 50 Mbit/s optical link operating over one meter. Future directions are then discussed.**

***Index Terms*— Beam-steering, liquid crystal, polarization grating, optical communication.**

I. Introduction

THERE is exponentially growing demand for wireless communications, with the majority being indoors. LiFi and optical wireless [1] is a maturing field of research with growing commercial interest, and has the potential to augment the capacity provided by RF wireless alone. Visible light communication (VLC) is capable of transmission rates in excess of 1 Gbit/s [2], [3] and hybrids of WiFi and VLC have also been demonstrated [4].

In order to increase data rates in excess of Gbit/s, optical wireless links must operate with a relatively narrow field of view, and in these circumstances, beam-steering is required to maintain a link over a wide coverage area. This is required at both transmitter and receiver in order to maximize the performance of the link. At the transmitter, beam-steering ensures the narrow beam of light reaches the receiver, and at the receiver beam-steering steers the incoming light 'back' onto the optical axis of the receiver. This allows the receiver to be designed with a large collection area and a narrow field of view.

Mechanical beam-steering is typically implemented using the movement of prisms and mirrors (for example [5]), although recently new MEMs-based approaches that change transmitter source position have been demonstrated [6]. Non-mechanical techniques include variable focus lenses [7], passive diffractive optics [8], integrated optical phased arrays [9] and/or tunable lasers [10]. These approaches typically offer beam-steering over a continuous set of angles and therefore require complex control and tracking arrangements to optimise alignment and achieve minimum link loss. In this letter, we present a simpler approach inspired by prior research [11] which focuses on discrete position beam-steering using polarization gratings and liquid crystal (LC) polarization shifters. Building upon this foundation, we implement a diffuser at the transmitter to obtain continuous angular coverage, as well as beam-steering at both the transmitter and receiver, which significantly improves the overall field of view compared to one that only uses beam-steering at the transmitter. Although the steering positions are discrete, the power at these positions can be tuned continuously. This approach also offers the potential for bidirectional communications since beam-steering is conducted for both the transmitter and receiver such that transmission no longer depends on the direction.

This letter is organized as follows: A brief introduction to polarization gratings is given, and then the system is described. Experimental details are provided and the result is detailed. Conclusions and future work complete the letter.

II. Theory

Polarization gratings (PGs) have periodic anisotropy across the plane which can change the phases of transmitted electric field components in one specific dimension leading to diffraction that is dependent on the polarization state of the illuminating wavefront [12]. For instance, a right-handed circularly polarized beam would be steered to the -1 order while a left-handed beam to the $+1$ order and a linearly polarized light to both states with divided intensities. Besides the primary beam upon diffraction, spots at other states can also be observed in experiments. These additional spots, which possess significantly lower intensities compared with the primary beam, have been reported by previous research that can be divided into three categories: zero-order, sub-order,

Manuscript received 22 July 2023; revised 14 August 2023; accepted 18 August 2023. Date of publication 5 September 2023; date of current version 11 September 2023. This work was supported in whole or in part by UKRI under Grant EP/X525777/1 for an Impact Acceleration Project. *(Corresponding author: Dominic O'Brien.)*

The authors are with the Department of Engineering Science, University of Oxford, OX1 3PJ Oxford, U.K. (e-mail: stephen.morris@eng.ox.ac.uk; dominic.obrien@eng.ox.ac.uk).

Color versions of one or more figures in this letter are available at https://doi.org/10.1109/LPT.2023.3308774.

Digital Object Identifier 10.1109/LPT.2023.3308774

and opposite-order spots, with an explanation and theoretical analysis of their appearance [13].

In conjunction with the PGs, planar-aligned nematic LC cells are used as tunable waveplates. The birefringence of nematic LCs changes continuously with the magnitude of applied voltage, which gives rise to a voltage-controlled waveplate that can alter the polarization state of the incident light. This approach is based on the concept proposed by J. Kim et al. [11]. The laser beam is initially polarized by the polarizer placed at a 45° angle to the direction of the first LC cell. A voltage is applied to adjust the polarization of the beam to either left or right circular polarization, or a combination of these. The first PG then steers the light according to this. The second LC cell then converts the state to either left or right circular or a combination, where the second PG then directs the light according to the input state.

A holographic diffuser is placed after the second PG and is used to expand the beam. This allows continuous angular coverage, whilst also ensuring eye-safety requirements can be met. To investigate the impact of the diffuser on the polarisation state of the beam, it was placed under a microscope with crossed polarizers and it was observed that the intensity of the microscope image changed with an in-plane rotation of the diffuser and the dark state appeared every 90° of rotation. In addition, the brightness of the microscope image remained unchanged for the same experiment when the polarizer after the diffuser was removed. This result indicates that the diffuser possesses a constant birefringence across the film, and the diffusion is independent of the input polarization state.

Light from the diffuser propagates to the receiver. Here an LC waveplate is used to convert the beam to be either left or right circularly polarized. It is then steered by the first PG so that the angle it subtends with the optical axis of the receiver is reduced, effectively reversing the steering effect of the corresponding transmitter PG. The light then passes through the second LC waveplate and PG, where it is steered in the other axis by the same process, again reducing the angle it subtends with the optical axis. The steered beam is then collected by the receiver. The receiver could be removed from the configuration and its position adjusted within the field of view.

There are substantial benefits to the approach described above, even for modest numbers of steering positions. Firstly, the approach is, in principle, agnostic to the transmission rate and the wavelength (provided the PG is designed for operation at the desired wavelength). Thus, there is no transmission bandwidth for the beam-steering system. In terms of the steering bandwidth, it is a function of the LC response time, where the LC waveplates used are measured to be 170 ms. As each of the steered positions covers an angular range of 10°, this response time would support rates of 58.82°/sec, sufficient for many situations with mobile terminals. Besides, through careful choice of the LC and using techniques such as polymer stabilization, a response time of the order of a few milliseconds can be obtained [14] which leads to a higher steering bandwidth. Secondly, the approach requires no mechanical components, is lightweight and compact, and can provide full space coverage. Thirdly, for a system where the desired angular coverage is $\psi \times \psi$ degrees, the transmitter and receiver would be optimally designed with the same field of view. If beam-steering to $N \times N$ positions are available at the transmitter, then the intensity at the receiver increases by N^2 compared with an unsteered system with the same overall field of view and transmitter power (if all light is diverted to a single position). If receiver beam-steering is implemented, then the required field of view of the receiver is $(\psi/N) \times (\psi/N)$ degrees. This allows an increase in receiver collection area by a factor of N^2 if the design is etendue limited (representing the best possible receiver design). Combining the effect of both transmitter and receiver steering leads to a potential overall N^4 gain in system link margin. This increased margin can be used to increase the link rate or range, or both, compared with the unsteered link.

III. Experiment

A schematic diagram of the experimental system for a free-space optical communication link based on PGs and LC wave-plates is shown in Fig. 1(a). An arbitrary waveform generator (81150A, Agilent) modulates a laser diode (LP520-SF15A, Thorlabs) powered by a laser driver (LDC205C, Thorlabs). The experimental apparatus limited the modulation index to 25% (where the modulation index is defined as the magnitude of optical power modulation relative to the maximum optical power). The laser beam is coupled into an optical fibre which runs through a polarization controller (FPC030, ThorLabs) before being connected to a collimator (F810FC-543, ThorLabs). The laser beam is then linearly polarized using a polarizer and then passes through the first LC cell.

The LC cells consist of a nematic LC mixture (E7, Synthon Chemicals Ltd) capillary filled into commercially available anti-parallel rubbed glass cells (LC-2, Instec) coated with indium-tin-oxide electrodes and polyimide alignment layers. The LC layer is 5 μm thick. The PGs (Edmund Optics) are designed to operate at 550 nm with a diffraction angle of ±10°, so there is a small amount of undiffracted light due to the mismatch with the laser wavelength (520 nm) [13].

Light is steered by the combination of the LC cell and PG, and then the second pair of devices is used to steer the beam in the orthogonal axis, leading to four potential steering positions. A light-shaping diffuser (P1, Luminit) then diffuses the beam into a 10° (FWHM) Lambertian intensity profile. Appropriate voltage control of the LC waveplates allows for addressing all four output regions (top-left, top-right, bottom-left, and bottom-right). The overall power transmitted after the diffuser was measured to be −6 dBm by a power meter. Combined with the modulation depth available, this leads to a mean modulated power (i.e. the useful communications power) of −12 dBm.

To investigate the spatial coverage of this system, a screen was temporarily placed in front of the receiver, and the voltages applied to the LC cells were adjusted so as to steer the diffused beam to all four regions simultaneously. The beam profile shown on the screen was captured by a CCD camera (DCU224C, Thorlabs) and is shown in Fig. 1(b). Note that

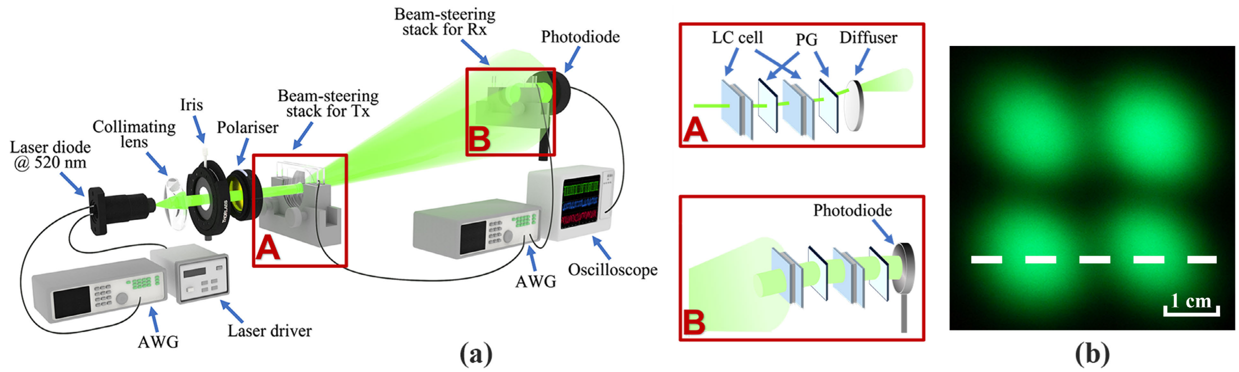

Fig. 1. (a) A schematic diagram of the free space optical communication link. A 520 nm laser diode is modulated by an arbitrary waveform generator (AWG). Four LC cells are individually driven by a second AWG. All electrical connections are represented by black lines and the optical path is in green. The components of each beam-steering stack and light propagation within the stacks are illustrated next to the schematic in the red boxes A (Transmitter, Tx, stack) and B (Receiver, Rx, stack). (b) The beam profile of all four steering states at the output of the transmitter is recorded on a screen by a CCD camera (DCU224C, Thorlabs). Setting the voltage of the LC cells accordingly allows for control of the power distribution of each steering region individually and simultaneously. Diffusers with larger diffusing angles can be employed to reduce the gap between each region. The white dashed line represents the direction in which the receiver was translated for the displacement measurement when the beam was steered to the bottom-left and bottom-right simultaneously.

the small gaps between each region are due to the camera not capturing the lower-intensity regions.

The insertion loss of the transmitter steering elements (after the initial polarizer that controls the polarization from the laser to after the diffuser at the output of the transmitter steerer) was measured to be 3.07 dB. This loss is predominantly caused by Fresnel reflections between the components and could be significantly reduced by index matching between the elements.

The receiver is designed as a combination of two LC cells, two PGs, and a PIN photodiode-based receiver. The LC cells and PGs steer the beam back towards the optical axis of the receiver and the receiver collects light and converts it to an electrical signal. The characteristics of the photodiode are detailed in [15], with an effective collection diameter of 20 mm and a field of view of at least 7° (half-angle), providing a reasonable match to the diffuser and PG angular characteristics.

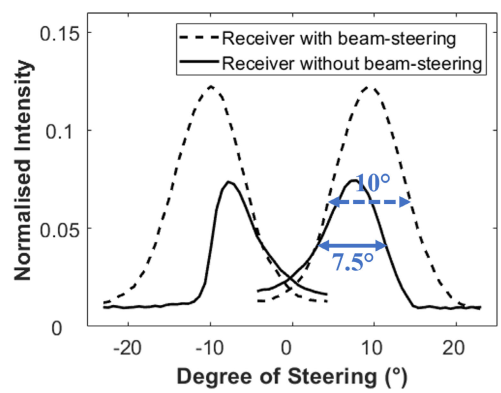

Fig. 2. Displacement measurements with and without the beam-steering stack at 40 cm distance from the transmitter. Both curves have been normalized to the transmitter output power allowing for an estimate of the geometrical link loss. The field of view of the individual steered beams (labelled in the figure) is estimated by measuring the FWHM of the normalized intensity curves. Results show that the beam-steering stack increases the effective detection angles and intensities of the received signal.

IV. Results and Discussion

Measurements were taken to show the benefits of active steering at both the transmitter and receiver. The transmitter beam was steered separately to the bottom left and bottom right positions, and in each case, the receiver was manually displaced and scanned across the center of the received pattern - as indicated by the dashed line in Fig. 1(b), and the received signal (equivalent to the optical power) recorded. Fig. 2 shows the power normalized to the power measured after the diffuser, giving an indication of the geometric loss of the link. In the case of the solid lines, it can be seen that the overall field of view is limited by the receiver field of view (7.5° half-angle). The dotted lines show the benefit of receiver beam-steering, with significant increases in signal and field of view relative to the case without steering. As mentioned previously, the dip in the received signal along the optical axis can be reduced by optimizing the relative receiver field of view, diffuser beam angle, and diffraction angle of the polarization grating.

Data transmission experiments were conducted over various link distances and the corresponding received signals were captured by an oscilloscope. A 50 Mbit/s non-return to zero on-off-keying pseudo-random binary sequence (PRBS) signal was used to test the link. Besides the point-to-point scenario, the transmitter was also set to a point-to-two-point scenario in which the output power was split 50/50 between the bottom-left and bottom-right regions. The corresponding BER was estimated using the complementary error function and the Q factor with μ_0, μ_1 being the mean voltages associated with the transmission states and σ_0, σ_1 the corresponding standard deviation of the noise (labelled on Fig. 3).

$$\mathrm{BER} = 0.5\ \mathrm{erfc}(Q/\sqrt{2}) \tag{1}$$

$$Q = \frac{\mu_1 - \mu_0}{\sigma_1 + \sigma_0} \tag{2}$$

The results for the BER as a function of the received power at different link distances in both scenarios are presented in Fig. 3. A link distance of over 1 meter at a BER lower than 10^{-3} was achieved for the point-to-point link. This was reduced to 80 cm for the point-to-two-point scenario.

The difference in the average modulation power between both scenarios with the same BER is 3 dB, corresponding

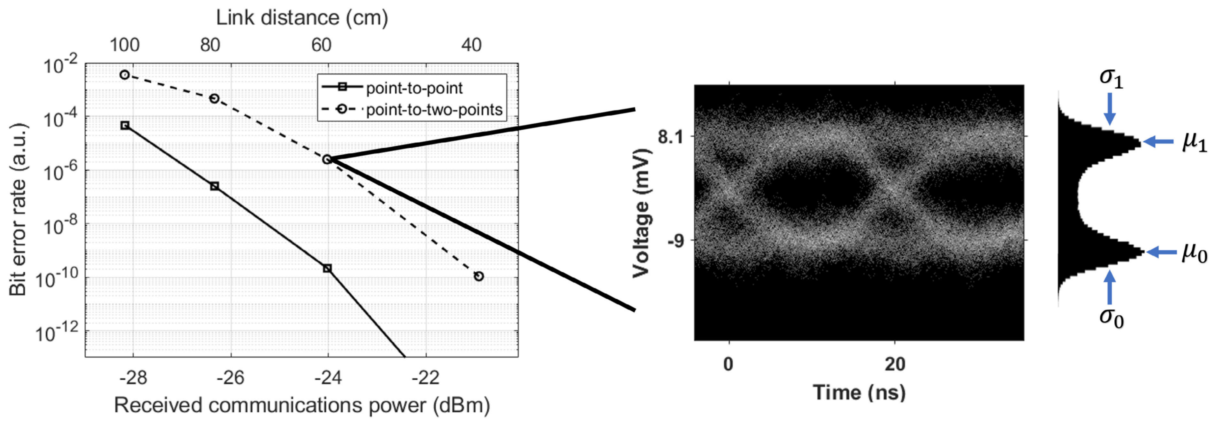

Fig. 3. The BER measured as a function of the average of the modulated power after the beam-steering and link distances in the point-to-point and point-to-two-point scenarios. The transmission rate was fixed to 50 Mbit/s. The eye diagram for the 60 cm link distance in the point-to-two-point scenario is shown highlighting the histogram used for the BER estimation.

to the split in energy between the two spatial regions. An eye diagram for a 60 cm, point-to-two-point scenario is also shown in Fig. 3 illustrating the noise distribution. The link distance can be further increased by employing a post amplifier or a fixed gain amplifier to the receiver. Furthermore, a higher transmission rate can be achieved by using a decision feedback equalizer since the receiver bandwidth limits the maximum transmission rate.

V. Conclusion

We successfully demonstrated a non-mechanical voltage-controlled beam-steering system for optical wireless communication using beam-steering at both transmitter and receiver. Results show that this approach offers a substantial increase in the field of view and link margin over using transmitter beam-steering alone. In principle, the beam-steering system can be designed for any transmission rate and wavelength, providing a considerable degree of flexibility. For the purposes of demonstration, we present a link transmitting 50 Mbit/s PRBS signals for over 1 meter with a BER lower than 10^{-3} for the point-to-point scenario.

Overall this beam-steering approach offers substantial improvements in link performance using potentially low-cost compact components that can be integrated to create a lightweight high-performance steering subsystem potential for a wide range of applications. Further work to demonstrate longer ranges, as well as further steps towards a bidirectional steered link, is underway.

Acknowledgment

The authors would like to thank Lin Ye for her support.

For the purpose of open access, the authors have applied a creative commons attribution (CC BY) licence (where permitted by UKRI, 'open government licence' or 'creative commons attribution no-derivatives (CC BY-ND) licence' may be stated instead) to any author accepted manuscript version arising.

References

[1] H. Haas, L. Yin, Y. Wang, and C. Chen, "What is LiFi?" *J. Lightw. Technol.*, vol. 34, no. 6, pp. 1533–1544, Mar. 15, 2016.

[2] A. M. Khalid, G. Cossu, R. Corsini, P. Choudhury, and E. Ciaramella, "1-Gb/s transmission over a phosphorescent white LED by using rate-adaptive discrete multitone modulation," *IEEE Photon. J.*, vol. 4, no. 5, pp. 1465–1473, Oct. 2012.

[3] R. X. G. Ferreira et al., "High bandwidth GaN-based micro-LEDs for multi-Gb/s visible light communications," *IEEE Photon. Technol. Lett.*, vol. 28, no. 19, pp. 2023–2026, Oct. 1, 2016.

[4] X. Wu, M. D. Soltani, L. Zhou, M. Safari, and H. Haas, "Hybrid LiFi and WiFi networks: A survey," *IEEE Commun. Surveys Tuts.*, vol. 23, no. 2, pp. 1398–1420, 2nd Quart., 2021.

[5] R. Singh et al., "Design and characterisation of terabit/s capable compact localisation and beam-steering terminals for fiber-wireless-fiber links," *J. Lightw. Technol.*, vol. 38, no. 24, pp. 6817–6826, Dec. 15, 2020.

[6] D. A. Goldman et al., "MOEMS-based lens-assisted beam steering for free-space optical communications," *J. Lightw. Technol.*, vol. 41, no. 9, pp. 2675–2690, May 1, 2023.

[7] V. Mai and H. Kim, "Non-mechanical beam steering and adaptive beam control using variable focus lenses for free-space optical communications," *J. Lightw. Technol.*, vol. 39, no. 24, pp. 7600–7608, Dec. 15, 2021.

[8] C. W. Oh, Z. Cao, E. Tangdiongga, and T. Koonen, "Free-space transmission with passive 2D beam steering for multi-gigabit-per-second per-beam indoor optical wireless networks," *Opt. Exp.*, vol. 24, no. 17, pp. 19211–19227, Aug. 2016.

[9] C.-W. Chow et al., "Actively controllable beam steering optical wireless communication (OWC) using integrated optical phased array (OPA)," *J. Lightw. Technol.*, vol. 41, no. 4, pp. 1122–1128, Feb. 15, 2023.

[10] L. Wu, Y. Han, Z. Li, Y. Zhang, and H. Y. Fu, "12 Gbit/s indoor optical wireless communication system with ultrafast beam-steering using tunable VCSEL," *Opt. Exp.*, vol. 30, no. 9, pp. 15049–15059, Apr. 2022.

[11] J. Kim, C. Oh, M. J. Escuti, L. Hosting, and S. Serati, "Wide-angle non-mechanical beam steering using thin liquid crystal polarization gratings," in *Proc. SPIE*, J. D. Gonglewski, R. A. Carreras, and T. A. Rhoadarmer, Eds. vol. 7093, 2008, pp. 1–12.

[12] C. Hoy, J. Stockley, J. Shane, K. Kluttz, D. McKnight, and S. Serati, "Non-mechanical beam steering with polarization gratings: A review," *Crystals*, vol. 11, no. 4, p. 361, Mar. 2021.

[13] G. Zhang et al., "Non-mechanical optical beam-steering of a liquid crystal laser," *Opt. Laser Technol.*, vol. 157, Jan. 2023, Art. no. 108623.

[14] Y. Jin et al., "Millisecond optical phase modulation using multipass configurations with liquid-crystal devices," *Phys. Rev. Appl.*, vol. 14, no. 2, Aug. 2020, Art. no. 024007.

[15] S. Khoo, "Eyesafe optical link using a holographic diffuser," in *Proc. IEE Colloq. Opt. Wireless Commun.*, 1999, p. 3.